行政院國家科學委員會專題研究計畫　期中進度報告

子計畫四:同步、通道估計與內接收機設計(1/2)

計畫類別： 整合型計畫
計畫編號： NSC94-2213-E-009-056-
執行期間： 94 年 08 月 01 日至 95 年 07 月 31 日
執行單位： 國立交通大學電信工程學系(所)

計畫主持人： 蘇育德

計畫參與人員： 林淵斌、王士瑋、楊哲雄、陳慧珊、王琬瑜

報告類型： 精簡報告

處理方式： 本計畫可公開查詢

中　華　民　國 95 年 5 月 30 日

行政院國家科學委員會專題研究計畫成果報告

下一世代無線行動接取技術-子計畫四:同步、通道估計與內接收機設計(1/2)

Next Generation Mobile Radio Access Technologies : Synchronization, channel estimation and inner receiver design (1/2)

計畫編號：NSC 94-2213-E-009-056
執行期間： 94/08/01~95/07/31
主持人：蘇育德教授　國立交通大學電信工程學系
計畫參與人員：林淵斌、王士瑋、楊哲雄、陳慧珊、王琬瑜

中文摘要

正交分頻多工（Orthogonal Frequency Division Multiplexing, OFDM）技術近年來頗受重視，其應用範圍也越來越廣。OFDM 通訊系統之設計必須要考慮在載波頻率偏宜（CFO）補償這個重要的課題，因載波頻率偏移會破化次載波的正交性且將嚴重地降低系統效能。在此篇報告裡，我們首先證明摩斯氏（Moose）的最大可能頻率估計法可推廣到多輸入輸出正交分頻多工（MIMO-OFDM）系的頻率估計子系統中，並有相當突出的性能表現。我們為了降低複雜度，更利用 YS 的轉換域方法並將將它推廣至多天線 OFDM 系統，由模擬成果發現相當有效地簡化頻率同步估測的複雜度且同時提高其性能表現。此篇報告的目的是針對多輸入輸出的正交分頻多工系統的頻率同步問題去發展一個更有效率的解決方案。我們發現此計畫報告中的的兩種方法皆可有效地改良並適用於多輸入輸出的系統。

關鍵詞：多輸入輸出，正交頻率多工，載波頻率偏移估測、最大可能估測

Abstract

For orthogonal frequency division multiplexing (OFDM) based systems, a nonzero carrier frequency offset (CFO) between the transmitter and receiver destroy the orthogonality amongst subcarriers and degrades the performance. In this report, we extend Moose's maximum likelihood CFO estimation algorithm for multiple transmit and multiple receive MIMO-OFDM systems. In order to reduce the complexity of the CFO subsystem, we extend the transform domain approach of Yu and Su [10] to the MIMO-OFDM scenario. From simulation results, we find Yu's algorithm efficiently reduce the complexity of CFO subsystem in MIMO-OFDM system and simultaneously improve its performance The purpose of this report is find a more efficient solution for MIMO-OFDM frequency synchronization. We find it both feasible and convenient to extend two of the OFDM CFO ML estimation approaches to the MIMO scenario.

Keywords: MIMO, OFDM, Carrier Frequency Offset Estimation, Maximum Likelihood Estimation

1. Introduction

Orthogonal frequency division multiplexing (OFDM) is a popular modulation scheme for high-speed broadband wireless transmission [1], [2]. It popularity derives mainly from its capability to combat frequency selective fading as intersymbol interference (ISI) caused by multipath delay spread can be easily eliminated. By copying a properly selected portion (called a cyclic prefix) of an OFDM block and appending it to that block,

each data-bearing subcarrier experiences only at fading if the duration of the cyclic prefix is longer than the maximum channel delay spread and block length is smaller than the channel coherent time. Hence, complicated equalization can be replaced by an one-tap equalizer in frequency domain. OFDM has been adopted as the transmission scheme for industrial standards like the asymmetric digital subscriber line (ADSL), digital audio broadcasting (DAB), terrestrial digital video broadcasting (DVB-T), power-line transmission, and high-speed wireless broadband area networks (WLAN's). It is being considered, among others, for air interface standards in IEEE 802:15n personal area network and 4G mobile network. The former adopts the Multiple Input Multiple Output (MIMO) technique to enhance the capacity, where MIMO refers to systems that have multiple transmit antennas and multiple receive antennas. Depending on the MIMO channel condition, the capacity of MIMO system increases with the number of transmitter and receive antennas. Recent developments in MIMO techniques promise a great boost in performance for OFDM systems.

With all its merits, OFDM, however, is sensitive to the carrier frequency offset (CFO) caused by Doppler shifts or instabilities of and mismatch between transmitter and receiver oscillators [3]. Depending on the application, the offset can be as large as many tens subcarrier spacing, and is usually divided into integer and fractional CFO parts.

The presence of a fractional CFO causes reduction of amplitude of desired subcarrier and induces inter-carrier interference (ICI) because the desired subcarrier is no long sampled at the zero-crossings of its adjacent carriers' spectrum. If the fractional CFO part can be perfectly compensated, the residual integer CFO does not degrade the signal quality but still results in circular shifts of the desired output, causing decision errors.

There have been a multitude of proposals for CFO compensation. A maximum likelihood estimate was proposed by Moose [4], based on the observation of two consecutive and identical symbols. Its maximum frequency acquisition range is only 1/2 subcarrier spacing because of mod 2π ambiguity. Two training symbols are also employed by Schmidl and Cox [5]. The first has two identical halves and serves to measure the frequency offset with an ambiguity equal to the subcarrier spacing. The second contains a pseudonoise sequence and its used to resolve the ambiguity, i.e. estimate integer CFO. Morelli *et al*, [6] suggested an estimate based on the observation of two consecutive symbols. This method overcomes the the ambiguity due to phase uncertainty but requires heavier computational load. Combining the advantages of OFDM and MIMO techniques, a variety of MIMO-OFDM architectures techniques have been proposed. Much less literature on the corresponding time and frequency synchronization and channel estimation issues can be found though [7-9].

The rest of the report is organized as follows. Section 2 describes system model and signal description for CFO of MIMO-OFDM system. In Section 3.1, we extend Moose's ML CFO estimation algorithm for use in a multiple-antenna environments, assuming two identical pilot symbols are available. In Section 3.2, we then extend the Yu and Su (YS) ML CFO estimation algorithm [10] that uses multiple repetitive pilot symbols. In Section 4, we show our simulation results and discussion

to verify the proposed algorithm.

2. System Model

2.1 Conventional OFDM System Model Description

Fig. 1 plots a block diagram of a OFDM modulator where S/P and DAC are used to denote serial-to-parallel converter and digital-to-analog converter, respectively. The information symbols are used to modulate subcarriers via an N-point inverse discrete Fourier transform (IDFT). The output of the IDFT (IFFT) block is converted to a serial complex block and a cyclic prefix (CP) is added to each block. The total duration of an OFDM symbol (frame) is equal to the length of the CP plus that of the IDFT symbol block. The CP is a copy of the tail part of the time-domain OFDM block and is attached to the front of the block. As long as the duration of the CP is longer than the channel impulse response, intersymbol inference (ISI) can be eliminated by the receiver through frequency domain excision. An OFDM demodulator is shown in Fig. 2. Based on the timing (frame) recovery subsystem output, the baseband receiver removes the CP part, takes discrete Fourier transform (DFT) on the remaining part and then compensates for the CFO and channel effect using information given by the frequency synchronization and channel estimation units before making decision on symbols modulated on each subcarrier, if no soft-decision channel decoding is needed. Parallel-to-serial conversion can be performed either before or after making symbol decision (detection). Fig. 3 depicts a MIMO-OFDM system with M_T transmit antennas and MR receive antennas. System design consideration prefers the choice of subcarrier spacing is such that each subcarrier suffers only slow flat fading. The resulting MIMO-OFDM channel can thus be characterized by a family of matrices whose members specify the space transmission characteristic, i.e., the (*i; j*) entry of a member matrix represents the channel response between the *i*th receive antenna and the *j*th transmit antenna associated with a subcarrier. One can also use a tensor to describe the space-frequency channel responses. The carrier frequency offset (CFO) is caused by (i) the time-varying nature of the transmission medium, (ii) the instabilities and mismatch between the transmitter and receiver oscillators and (iii) the relative movement between the transmitter and receiver. For all practical purpose, different transmit/receive RF branches of a MIMO system must be frequency-coherent, i.e., the transmitted carrier frequency and receiver frequency down-converters are each derived from a common frequency synthesizer, resulting in the model shown in Fig. 4. The cyclic prefix (CP) consists of Ng samples, which is supposed to be greater than or equal to the maximum relative delay that includes users' timing ambiguities and the maximum multipath delay; see Fig. 5. When this assumption is valid, the received time-domain sequence, after removing the CP part, is the circular convolution of the transmitted sequence with the channel impulse response plus white Gaussian noise.

2.2 MIMO-OFDM System Model and Signal Descriptions

Consider a frequency selective fading channel associated with a MIMO system of M_T transmit and M_R receive antennas. The equivalent time-domain baseband signal at the output of the *i*th receive antenna, $y_i[n]$, is given by

$$y_i[n] = \sum_{j=1}^{M_T} r_{i,j}[n] + w_i[n];\ n = 1, 2, ..., N;\ i = 1, 2, ..., M_R \quad (1)$$

where $\{w_i[n]\}$ is a complex additive whit Gaussian noise (AWGN) sequence and

$$r_{i,j}[n] = \frac{1}{N} \sum_{k \in D_j} \sqrt{\frac{E_s}{M_T}} S_j[k] H_{i,j}[k] e^{j2\pi n(k+\epsilon)/N} \quad (2)$$

is the part of the OFDM signal received by the *i*th receive antenna contributed by the *j*th transmit antenna. Moreover,

- $S_j[k]$ represents the symbol carried by the *k*th subcarrier at the *j*th transmit antenna.
- $H_{i,j}[k]$ is the channel transfer function between the *i*th receive antenna and the *j*th transmit antenna at the *k*th subcarrier.
- ε denotes the relative carrier frequency offset of the channel (the ratio of the actual frequency to the intercarrier spacing).
- D_j is the set of modulated subcarrier for the *j*th transmit antenna.
- E_s is the average energy allocated to the *k*th subcarrier evenly divided across the transmit antennas.
- $\{h_{i,j}[n]\}$ and $H_{i,j}[k] = \sum_{n=0}^{L-1} h_{i,j}[n] e^{-\frac{j2\pi kn}{N}}$ are the channel impulse and frequency response between the *i*th receive antenna and the *j*th transmit antenna at the *k*th subcarrier.
- L is the maximum channel memory of all $M_T M_R$ SISO component channels.

Fig. 6 plots the transmission channel model for the *i*th receive antenna with respect to the MT transmit antennas. Rewriting (2.1) in matrix form

$$\begin{pmatrix} y_1[n] \\ y_2[n] \\ \vdots \\ y_{M_R}[n] \end{pmatrix} = \frac{1}{N} \sum_{k \in D_j} \sqrt{\frac{E_s}{M_T}} \begin{pmatrix} H_{1,1}[k] & H_{1,2}[k] & \cdots & H_{1,M_T}[k] \\ H_{2,1}[k] & H_{2,2}[k] & \cdots & H_{2,M_T}[k] \\ \vdots & \vdots & \ddots & \vdots \\ H_{M_R,1}[k] & \cdots & \cdots & H_{M_R,M_T}[k] \end{pmatrix} e^{j2\pi n(k+\varepsilon)/N} + \begin{pmatrix} w_1[n] \\ w_2[n] \\ \vdots \\ w_{M_R}[n] \end{pmatrix} \quad \textbf{(3)}$$

and using the substitutions

$$\mathbf{y}[n] = (y_1[n]\ y_2[n]\ \cdots\ y_{M_R}[n])^T$$
$$\mathbf{S}[k] = (S_1[k]\ S_2[k]\ \cdots\ S_{M_T}[k])^T$$
$$\mathbf{H}[k] = [H_{i,j}[k]]$$
$$\mathbf{w}[n] = (w_1[n]\ w_2[n]\ \cdots\ w_{M_R}[n])^T$$

we obtain

$$\mathbf{y}[n] = \frac{1}{N} \sum_{k \in D_j} \sqrt{\frac{E_s}{M_T}} \mathbf{H}[k] \mathbf{S}[k] e^{j2\pi n(k+\epsilon)/N} + \mathbf{w}[n] \quad (4)$$

Let ε_f and ε_i be respectively the fractional and integer parts of the CFO so that $\varepsilon = \varepsilon_f + \varepsilon_i$ and define

$$\begin{aligned} Y[k] &= \sqrt{\frac{E_s}{M_T}} \sum_{m \in D_j} H[m] S[m] \left(\frac{1}{N} \sum_{n=0}^{N-1} e^{j2\pi(m+\varepsilon_f+\varepsilon_i)n/N} e^{-j2\pi kn/N} \right) + W[k] \\ &= \sqrt{\frac{E_s}{M_T}} H[k-\varepsilon_i] S[k-\varepsilon_i] \left(\frac{1}{N} \sum_{n=0}^{N-1} e^{-j2\pi\varepsilon_f n/N} \right) \\ &\quad + \sqrt{\frac{E_s}{M_T}} \sum_{\substack{m \in D_j \\ m \neq k-\varepsilon_i}} H[m] S[m] \left(\frac{1}{N} \sum_{n=0}^{N-1} e^{j2\pi(m+\varepsilon_f-k)n/N} e^{j2\pi\varepsilon_f n/N} \right) + W[k] \\ &= \sqrt{\frac{E_s}{M_T}} \underbrace{H[k-\varepsilon_i] S[k-\varepsilon_i]}_{\text{circular shift}} \underbrace{\left(\frac{1}{N} \frac{\sin(\pi\varepsilon_f)}{\sin(\pi\varepsilon_f/N)} e^{-j2\pi\varepsilon_f(N-1)/N} \right)}_{\text{reduction of the desired subcarrier}} \\ &\quad + \underbrace{\sqrt{\frac{E_s}{M_T}} \sum_{\substack{m \in D_j \\ m \neq k-\varepsilon_i}} H[m] S[m] \left(\frac{1}{N} \frac{\sin(\pi(\varepsilon_f+\varepsilon_i))}{\sin(\pi(m-k+\varepsilon_f+\varepsilon_i)/N)} e^{j\pi(\varepsilon_f+\varepsilon_i)(N-1)/N} e^{-j\pi(m-k)/N} \right)}_{ICI} \\ &\quad + W[k] \end{aligned} \quad (6)$$

It is clear that the presence of a fractional CFO causes reduction of the desired subcarrier's amplitude and induces inter-carrier interference (ICI). If the fractional CFO part can be perfectly compensated for, the integer CFO, if exists, will result in a circular shift of the desired output, causing decision errors.

3. Maximum Likelihood Estimate of CFO

3.1 Generalized Moose Estimate

Let *D* be the set of modulated subcarrier (indexes) that bear a pseudonoise (PN) sequence on the even frequencies and zeros on the odd frequencies. The resulting time-domain training sequence has two identical halves

$$r[n]=\frac{1}{N}\sum_{k\in D_e}\sqrt{\frac{E_s}{M_T}}H[k]S[k]e^{j2\pi n(k+\varepsilon)/N} \qquad (7)$$

$$\begin{aligned} r[n+N/2] &= \frac{1}{N}\sum_{m\in D_e}\sqrt{\frac{E_s}{M_T}}H[k]S[k]e^{j2\pi(n+N/2)(k+\varepsilon)/N} \\ &= \frac{1}{N}\sum_{m\in D_e}\sqrt{\frac{E_s}{M_T}}H[k]S[k]e^{j2\pi n(k+\varepsilon)/N}e^{j2\pi\frac{N}{2}(k+\varepsilon)/N} \\ &= r[n]e^{j2\pi\varepsilon/2}\ ,\ n=1,2..,N/2 \end{aligned} \qquad (8)$$

where $\left(r_1[n] \quad r_2[n] \quad \cdots \quad r_{M_R}[n]\right)^T$ and D_e is the subset of even numbers in *D*.

Taking into account the AWGN term, we obtain

$$y[n]=r[n]+w[n] \qquad (9)$$

$$y[n+N/2]=r[n]e^{j2\pi\varepsilon/2}+w[n+N/2] \qquad (10)$$

where $\left(w_1[n] \quad w_2[n] \quad \cdots \quad w_{M_R}[n]\right)^T$. As illustrated in Fig 7, we define

$$\bar{\mathbf{y}}_1[i] = (y_i[1]\ y_i[2]\ \cdots\ y_i[N/2])$$

$$\bar{\mathbf{r}}_1[i] = (r_i[1]\ r_i[2]\ \cdots\ r_i[N/2])$$

$$\bar{\mathbf{w}}_1[i] = (w_i[1]\ w_i[2]\ \cdots\ w_i[N/2])$$

and

$$\bar{\mathbf{y}}_2[i] = (y_i[N/2+1]\ y_i[N/2+2]\ \cdots\ y_i[N])$$

$$\bar{\mathbf{r}}_2[i] = (r_i[N/2+1]\ r_i[N/2+2]\ \cdots\ r_i[N])$$

$$\bar{\mathbf{w}}_2[i] = (w_i[N/2+1]\ w_i[N/2+2]\ \cdots\ w_i[N])$$

where the subscript indicates either the first or the second half of a time-domain OFDM frame and the indexes within the bracket denotes from which receive antenna the time domain sample is derived.

(9) and (10) then have the simplified expressions

$$\bar{\mathbf{y}}_1[i] = \bar{\mathbf{r}}_1[i]+\bar{\mathbf{w}}_1[i] \qquad (11)$$

$$\bar{\mathbf{y}}_2[i] = \bar{\mathbf{r}}_1[i]e^{j2\pi\epsilon/2}+\bar{\mathbf{w}}_2[i] \qquad (12)$$

The ML estimate of the parameter ε, given the received vector $(\bar{y}_1[i],\bar{y}_2[i])$, is obtained by maximizing the likelihood function

$$f(\bar{y}_1[i],\bar{y}_2[i]\,|\,\varepsilon)=f(\bar{y}_2[i]\,|\,\bar{y}_1[i],\varepsilon)f(\bar{y}_1[i]\,|\,\varepsilon) \qquad (13)$$

where we have denoted various conditional probability density functions by similar functional expressions, *f*(.|.). As ε gives no explicit information about $\bar{y}_1[i]$, i.e. $f(\bar{y}_1[i]\,|\,\varepsilon)=f(\bar{y}_1[i])$, the ML estimate of ε is given by

$$\begin{aligned} \hat{\varepsilon} &= \arg\max_{\varepsilon} f(\bar{y}_2[i]\,|\,\bar{y}_1[i],\varepsilon)f(\bar{y}_1[i]\,|\,\varepsilon) \\ &= \arg\max_{\varepsilon} f(\bar{y}_2[i]\,|\,\bar{y}_1[i],\varepsilon) \end{aligned} \qquad (14)$$

Since

$$\begin{aligned} \bar{y}_2[i] &= (\bar{y}_1[i]-\bar{w}_1[i])e^{j2\pi\varepsilon/2}+\bar{w}_2[i] \\ &= \bar{y}_1[i]e^{j2\pi\varepsilon/2}+(\bar{w}_1[i]-\bar{w}_2[i]e^{j2\pi\varepsilon/2}) \end{aligned} \qquad (15)$$

and $\bar{w}_1[i],\bar{w}_2[i]$ are temporally white Gaussian with zero mean and variance $\sigma_w^2 I$, where ***I*** is the identity matrix, the multivariate Gaussian vector $\bar{y}_2[i]$ have mean $\bar{y}_1[i]e^{j2\pi\varepsilon/2}$ and covariance matrix

$$E[(\bar{\mathbf{w}}_2[i]-\bar{\mathbf{w}}_1[i]e^{j2\pi\epsilon/2})(\bar{\mathbf{w}}_2[i]-\bar{\mathbf{w}}_1[i]e^{j2\pi\epsilon/2})^H] = 2\sigma_w^2\mathbf{I} \qquad (16)$$

Then

$$\begin{aligned} \Lambda(\varepsilon) &= f(\bar{y}_1[1]\cdots\bar{y}_1[M_R],\bar{y}_2[1]\cdots\bar{y}_2[M_R]\,|\,\bar{y}_1[1]\cdots\bar{y}_1[M_R],\varepsilon) \\ &\propto \exp\left\{-\frac{1}{2\sigma_\omega^2}\sum_{i=1}^{M_R}\left(\bar{y}_2[i]-\bar{y}_1[i]e^{j2\pi\varepsilon/2}\right)\left(\bar{y}_2[i]-\bar{y}_1[i]e^{j2\pi\varepsilon/2}\right)^H\right\} \\ &\propto \exp\left\{\frac{1}{2\sigma_\omega^2}\sum_{i=1}^{M_R}2\Re\left\{\bar{y}_2[i]\bar{y}_1^H[i]e^{-j2\pi\varepsilon/2}\right\}\right\} \\ &= \exp\left\{\frac{1}{\sigma_\omega^2}\Re\left\{\left(\sum_{i=1}^{M_R}\sum_{n=1}^{M_R}y_i^*[n]y_i[n+N/2]\right)e^{-j2\pi\varepsilon/2}\right\}\right\} \end{aligned} \qquad (17)$$

The ML estimate of ε is given by

$$\begin{aligned}\hat{\epsilon} &= \arg\max_{\epsilon} \Lambda(\epsilon) \\ &= \frac{1}{\pi}\mathrm{Arg}\left(\sum_{i=1}^{M_R}\sum_{n=1}^{N/2} y_i^*[n]y_i[n+N/2]\right)\end{aligned} \quad (18)$$

where Arg(x) is the principal argument of the complex number x. In summary, the generalized Moose estimate for two identical halves pilot symbols of length N_w and N_D-spaced, as shown in Fig. 8, is given by

$$\hat{\epsilon} = \frac{N}{2\pi N_D}\mathrm{Arg}\left(\sum_{i=1}^{M_R}\sum_{n=1}^{N_W} y_i^*[n]y_i[n+N_D]\right) \quad (19)$$

The range of this estimator is $\pm\frac{N}{2N_D}$ subcarrier spacings.

3.2 Extended Yu-Su Estimate

Consider a MIMO-OFDM system that uses multiple identical pilot symbols. After discarding the first received symbol, the remaining *K* pilot symbols at the *i*th receive antenna, $y_i(k,m)$, can be represented as

$$y_i(k,m) = x_i(k,m) + w_i(k,m) \quad (20)$$

for $k=1,2,\ldots,K$ and $m=1,2,\ldots,M$, where $x_i(k,m)$ is the *m*th sample of the *k*th (time-domain) symbol of the channel output at the *i*th receiver antenna. $\{w_i(k,m)\}$ are uncorrelated circularly symmetric Gaussian random variables at the *i*th receive antenna with zero mean and variance $\sigma_w^2 = E\{|w_i(k,m)|^2\}$. Note that

$$x_i(k,m) = x_1(1,m)e^{j2\pi(k-1)M\varepsilon/N} \quad (21)$$

where ε is the relative frequency offset of the channel. Let

$$\begin{aligned}Y_i(m) &= [y_i(1,m) \cdots y_i(K,m)]^T \\ A(\epsilon) &= [1\ e^{j2\pi\epsilon M/N} \cdots e^{j2\pi\epsilon(K-1)M/N}]^T \\ W_i(m) &= [w_i(1,m) \cdots w_i(K,m)]^T\end{aligned} \quad (22)$$

where $(.)^T$ denotes the matrix transpose. $Y_i(m), A(\varepsilon)$ and $W_i(m)$ are the vectors of dimension *Kx1*. Then, as shown in Fig 9, we have

$$Y_i(m) = A(\varepsilon)x_i(1,m) + W_i(m), m = 1,\ldots,M \quad (23)$$

The received samples can thus be expressed compactly as $Y_i = A(\varepsilon)X_i + W_i$ where $Y_i = [Y_i(1)\cdots Y_i(M)]$ is an $K \times M$ matrix. $X_i = [x_i(1,1)\cdots x_i(1,M)]$ is an $1 \times$ M vector and $W_i = [W_i(1)\cdots W_i(M)]$ is an $K \times M$ matrix.

Since the noise is temporally whit Gaussian, $Y_i(m)$ is a multivariate Gaussian distributed random vector with covariance matrix $\sigma_w^2 I$.

The joint ML estimates of *A* and X_i, treating X_i as a deterministic unknown vector, are obtained by maximizing the following joint likelihood function:

$$f(Y_1\cdots Y_{M_R}\,|\,A, X_1\cdots X_{M_R}) = \prod_{i=1}^{M_R}\prod_{m=1}^{M} f(Y_i(m)\,|\,A, x_i(1,m))$$

$$\propto e^{-1/\sigma_w^2\sum_{i=1}^{M_R}\sum_{m=1}^{M}\|Y_i(m)-Ax_i(1,m)\|^2}$$

The corresponding log-likelihood function, after dropping constant and unrelated terms, is given by

$$\Lambda(A, x_i(1,m)) = \sum_{i=1}^{M_R}\sum_{m=1}^{M}\|Y_i(m)-Ax_i(1,m)\|^2 \quad (24)$$

For a given *A*, setting

$$\nabla_{x_i(1,m)}\|Y_i(m)-Ax_i(1,m)\|^2 = 0$$

we obtain the conditional ML estimate,

$$\hat{x}_i(1,m) = x_{LS_i}(1,m) = A^+Y_i(m) \quad (25)$$

where $A^+ = A^H/K$ and *H* denotes the Hermitian operation. By substituting the least-square solution, $x_{LS_i}(1,m)$, we obtain

$$\Lambda(A)=\sum_{i=1}^{M_R}\sum_{m=1}^{M}\left\|Y_i(m)-AA^{+}Y_i(m)\right\|^2=\sum_{i=1}^{M_R}\sum_{m=1}^{M}\left\|P_A^{\perp}Y_i(m)\right\|^2$$
$$=\sum_{i=1}^{M_R}\sum_{m=1}^{M}Y_i^H(m)P_A^{\perp}Y_i(m)=tr\left(P_A^{\perp}\sum_{i=1}^{M_R}\sum_{m=1}^{M}Y_i(m)Y_i^H(m)\right)$$
$$=M_RMtr\left(P_A^{\perp}\hat{R}_{YY}\right) \quad (26)$$

where $tr(.)$ denotes the trace of a matrix, $\hat{R}_{YY}=\frac{1}{M_RM}\sum_{i=1}^{M_R}\sum_{m=1}^{M}Y_i(m)Y_i^H(m)$, and $P_A^{\perp}=I-AA^{+}$. The desired CFO estimate is then given by

$$\hat{\varepsilon}=\arg\left\{\min_{\varepsilon}tr\left(P_A^{\perp}\hat{R}_{YY}\right)\right\}=\arg\left\{\max_{\varepsilon}tr\left(P_A\hat{R}_{YY}\right)\right\}$$
$$=\arg\left\{\max_{\varepsilon}A^H\hat{R}_{YY}A\right\} \quad (27)$$

Invoking an approach similar to that used by the MUSIC algorithm, we set $z=e^{j2\pi\varepsilon M/N}$ and define the parametric vector

$$A(z)=\begin{bmatrix}1 & z & z^2 & \cdots & z^{K-1}\end{bmatrix}^T, \quad (28)$$

so that the log-likelihood $\Lambda=A^H\hat{R}_{YY}A$ can be expressed as a polynomial of order *2K-1*,

$$\Lambda(z)=A(z)^H\hat{R}_{YY}A(z)=\sum_{n=-(K-1)}^{K-1}s(n)z^n, \quad (29)$$

where $s(n)=\sum_{i,j}\hat{R}_{YY}(i,j)$, for n = *j-i*, and *n=-K+1,…, K-1*. As the log-likelihood is a real smooth function of ε, taking derivative of $\Lambda\left(e^{j2\pi\varepsilon M/N}\right)$ with respect to ε and setting $\partial\Lambda\left(e^{j2\pi\varepsilon M/N}\right)/\partial\varepsilon=\dot{\Lambda}(\varepsilon)=0$, we obtain

$$F(z)-F^{*}(z)=0 \quad (30)$$

where $F(z)=\sum_{n=1}^{K-1}ns(n)z^n$ is a polynomial of order *K-1*. If $\{z_i\}$are the nonzero complex roots of $\dot{\Lambda}(z)$ then the desired estimate is given by

$$\hat{\varepsilon}=\frac{N}{j2\pi M}\ln\hat{z} \quad (31)$$

where $\hat{z}=\arg\{\max_{z_i}\Lambda(z)\}$.

We summarize the above ML estimation procedure as following.

1. Collect *K* received symbols from all receive antennas and construct the sample correlation matrix $\hat{R}_{YY}$, which is given by $\hat{R}_{YY}=\frac{1}{M_RM}\sum_{i=1}^{M_R}\sum_{m=1}^{M}Y_i(m)Y_i^H(m)$.

2. Calculate the coefficients of *F(z)* based on $\hat{R}_{YY}$ where $F(z)=\sum_{n=1}^{K-1}ns(n)z^n$, and $s(n)=\sum_{i,j}\hat{R}_{YY}(i,j)$ for *n = j-i*.

3. Find the nonzero unit-magnitude roots of $F(z)-F^{*}(z)=0$.

4. Obtain the CFO estimate from and $\hat{\varepsilon}=\frac{N}{j2\pi M}\ln\hat{z}$ and $\hat{z}=\arg\{\max_{z_i}\Lambda(z)\}$ where $\Lambda(z)=A(z)^H\hat{R}_{YY}A(z)$, $z=e^{j2\pi\varepsilon M/N}$, and $A(z)=\begin{bmatrix}1 & z & z^2 & \cdots & z^{K-1}\end{bmatrix}^T$.

The range of our estimator is ±*M/2* subcarrier spacings.

4. Simulation Results and Discussion

The computer simulation results reported in this section are obtained by using a pilot format the same as that of the IEEE 802.11a standard with a sample interval of 50 ns. The frequency-selective fading channel has sixteen paths with independent complex Gaussian distributed amplitudes and a exponentially decaying power delay profile with rms delay spreads of 50 ns. The tap coefficients are normalized such that the sum of the average power per channel is unity. The DFT size is *N*

= 64. The signal-to-noise ratio (SNR), defined as the ratio of the received signal power (from all MT transmitters) to the noise power at the *i*th receive antenna, is assumed to be the same or each receive antenna. For Moose estimate, the training part consists of two identical halves with length N_W = 32. The range of CFO estimator is ±1 subcarrier spacings. Fig. 10 shows the performance of generalized Moose CFO estimate for different number of transmit and receive antennas. Obviously, the MSE performance improves as the number of receive antennas, M_R, increases. Fig.11 presents the performance of extended YS estimate for different number of transmit and receive antennas. The training symbol has two identical halves with K = 2 and M = 32. The range of CFO estimator is ±1 subcarrier spacings. For training symbol with two identical repetition, the performance of extended Yu estimate is the same as the performance of generalized Moose's CFO estimate. Fig. 12 plots the performance of generalized Moose's CFO estimate with two identical halves with length N_W = 32 for different number of transmit and receive antennas. Similarly, the performance of CFO estimates is an increasing function of the number of the receive antennas. We divide roughly into four groups. The first group is M_R = 1;M$_T$ = 1; 2; 4; 8, the second is M_R = 2;M_T = 1; 2; 4; 8 and so on. For
first group, the performance of CFO estimate with M_R = 1; M_T = 8 is better than
with M_R = 1; M_T = 1 duo to transmit diversity. The last group with MR = 8 is
more close together than the ¯rst group with M_R = 1 duo to receive diversity. The
performance of CFO estimate for the second group, M_R = 2, is roughly 3dB better than
for the first group, M_R = 1, duo to two receive antennas received double energy than
single receive antenna. Fig.13 shows the performance of extended Yu estimate and generalized Moose estimate. The training symbols have 4 repetitions with K = 4 and M = 16. The training symbols for generalized Moose estimate are length N_W = 32 i.e. take first two training symbols as one training symbol and take last two training symbols as one training symbol. The range of generalized Moose's CFO estimator is ±1 subcarrier spacings. The range of extended Yu estimator is ±2 subcarrier spacings. For 4 identical pilots, the performance of extended YS estimate is better than that of the generalized Moose estimate because extend YS estimate use all information of the training symbols.

5. Conclusion

In this project, we have extended both Moose and YS maximum likelihood CFO estimation algorithms for use in MIMO-OFDM systems. As long as the length of cyclic prefix is greater than or equal to the maximum delay that accounts for the all users' timing ambiguities and channel multipath delays. The performance of both CFO estimates improves as the number of transmit/receive antennas increases. In other words, the presence of multiple antennas not only promise great capacity enhancement but entail performance improvement for the associated frequency synchronization subsystem.

6. Reference

[1] S. Weinstein, P. Ebert, “Data Transmission by Frequency-Division Multiplexing Using the Discrete Fourier Transform," *IEEE Trans. Commun*., vol. 19, pp. 628 - 634, Oct 1971.

[2] R. van Nee, G. Awater, M. Morikura, H. Takanashi, M. Webster, and K. Halford, “New high-rate wireless LAN standards," *IEEE Commun. Mag*., vol. 37, pp. 82-88, Dec. 1999.

[3] T. Pollet, M. Van Bladel, M. Moeneclaey, "BER sensitivity of OFDM systems to carrier frequency offset and Wiener phase noise," *IEEE Trans. Commun*., vol. 43, pp. 191-193, Feb./March/April 1995.

[4] P. H. Moose, "A technique for orthogonal frequency division multiplexing frequency offset correction," *IEEE Trans. Commun*., vol. 42, pp. 2908-2914, Oct. 1994.

[5] T. M. Schmidl and D. C. Cox, "Robust frequency and timing synchronization for OFDM," *IEEE Trans. Commun.*, vol. 45, pp. 1613-1621, Dec. 1997.

[6] M. Morelli, A. N. DAndrea, and U. Mengali, "Frequency ambiguity resolution in OFDM system," *IEEE Commun. Lett*., vol. 4, pp. 134-136, Apr. 2000.

[7] A.N. Mody, G.L. Stuber, "Synchronization for MIMO OFDM systems," in *Proc. IEEE GlobalCom'01*, vol. 1, pp. 25-29, Nov. 2001.

[8] A.N. Mody, G.L. Stuber, "Receiver implementation for a MIMO OFDM system," in *Proc. IEEE GlobalCom'01*., vol. 1, pp. 17-21, Nov. 2002.

[9] Y. Asai, S. Kurosaki, T. Sugiyama, M. Umehira, "Precise AFC scheme for performance improvement of SDM-COFDM," IEEE Vehicular Tech., vol. 3, pp. 24-28, Sept. 2002.

[10] J.-H. Yu and Y. T. Su, "Pilot-assisted maximum likelihood frequency estimation for OFDM systems," *IEEE Trans. Commun*., pp. 1997-2004, Nov. 2004.

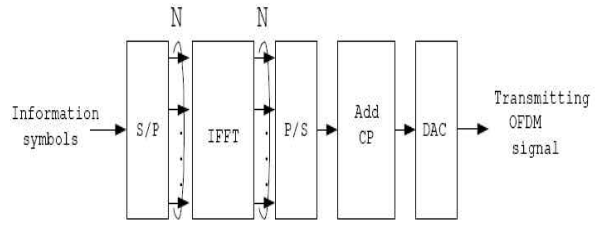

Figure 1：Block diagram of an OFDM modulator.

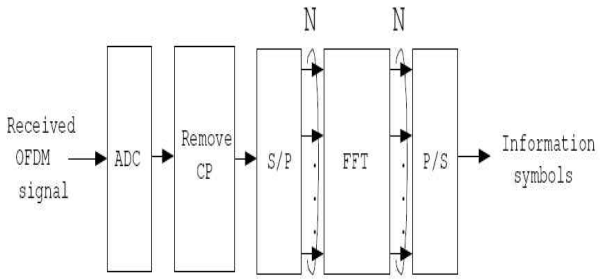

Figure 2：A typical OFDM demodulator.

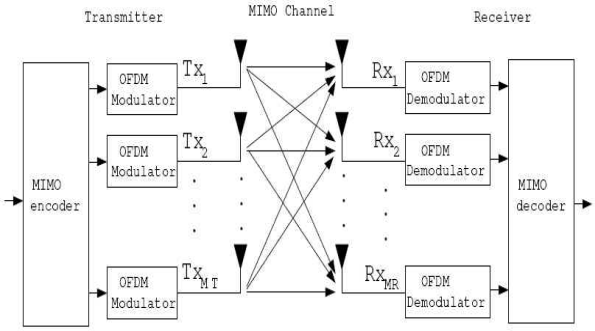

Figure 3：Block diagram of a typical MIMO-OFDM system.

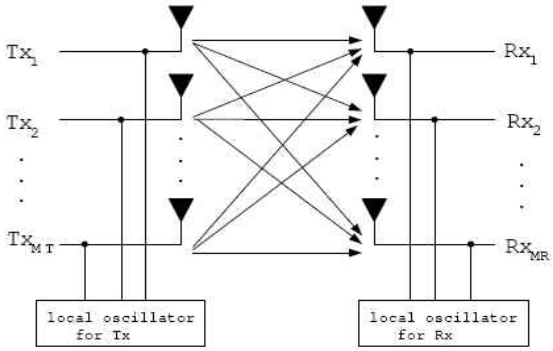

Figure 4：Frequency synthesizer model of a MIMO-CDMA system.

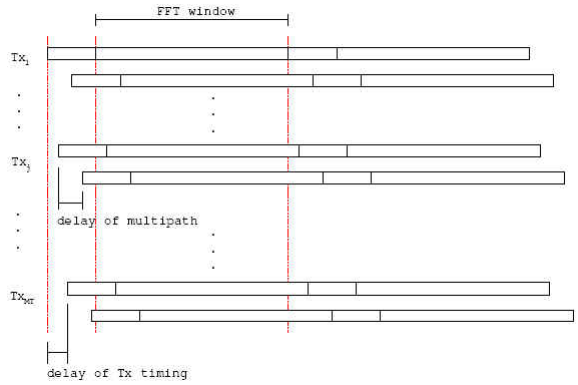

Fig. 5: Timing assumption of the MIMO-OFDM receiver under consideration.

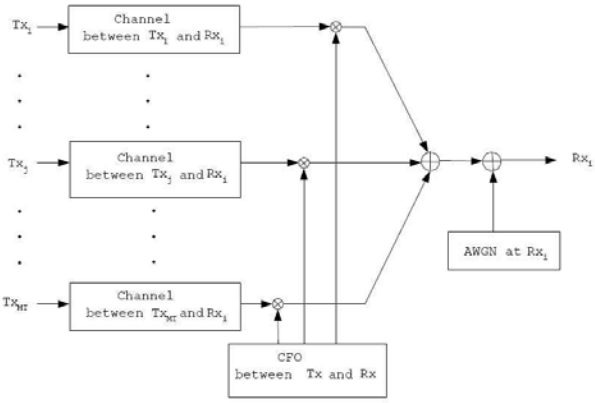

Fig. 6: Channel model for the ith receive antenna.

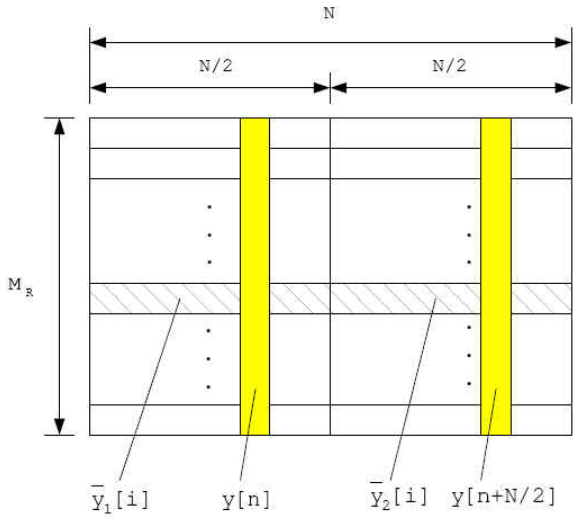

Fig. 7: Definitions of various vector notations.

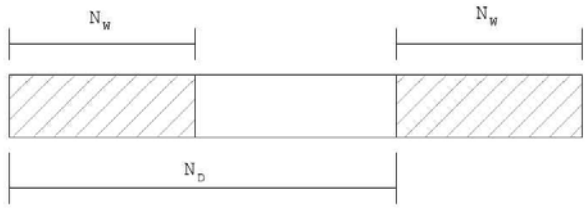

Fig. 8: The ND-spaced estimator.

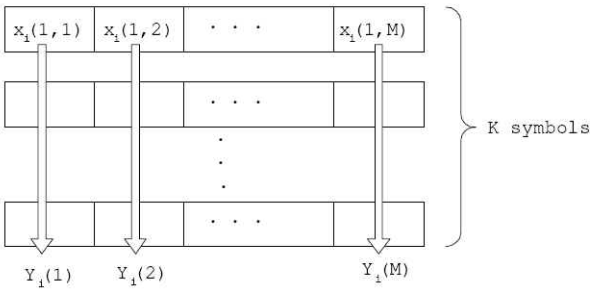

Fig. 9: Symbol arrangement and de¯nitions of the extended Yu's ML estimate at the ith receive antenna.

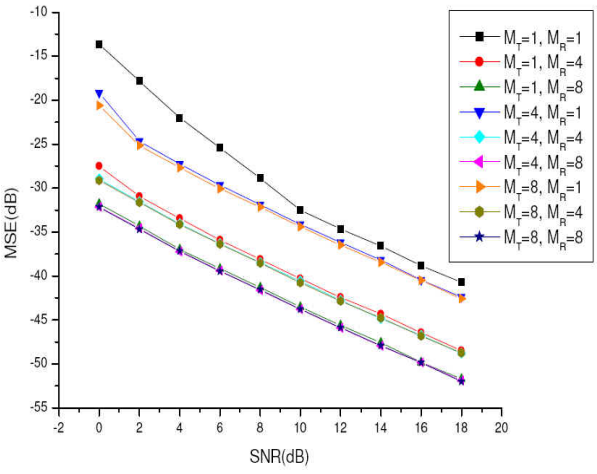

Fig. 10: MSE performance of generalized moose estimate for two repetitions, true CFO=0:7 subcarrier spacings.

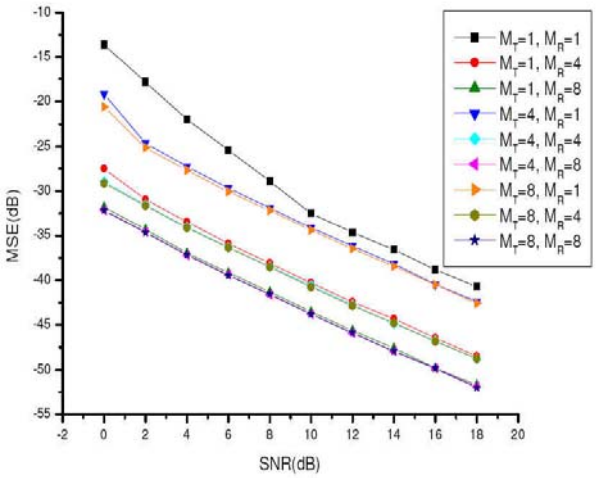

Fig. 11: MSE performance of extended Yu estimate for two repetitions, true CFO=0:7 subcarrier spacings.

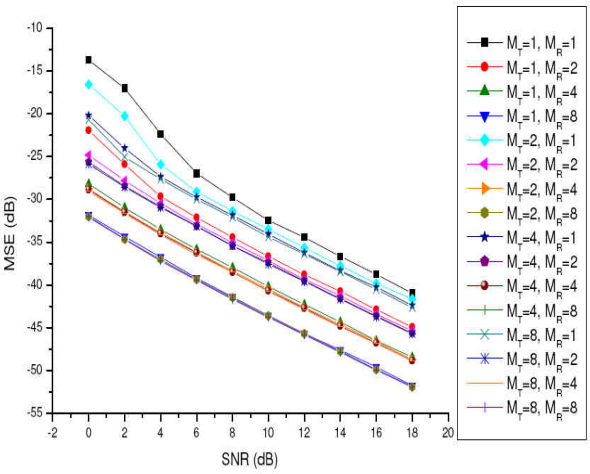

Fig.. 12: MSE performance of generalized moose estimate for two repetitions, true CFO=0:7 subcarrier spacings.

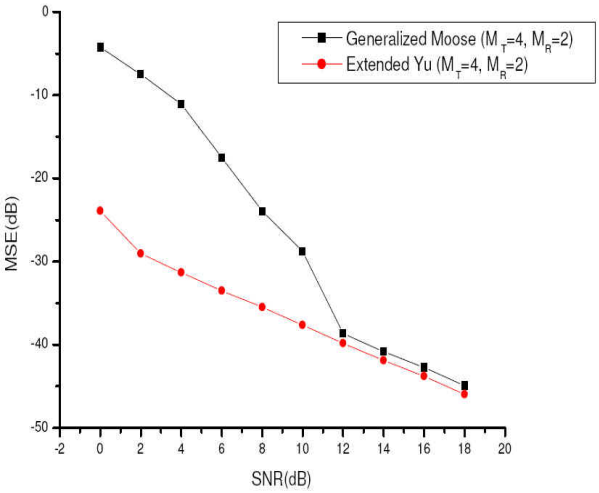

Fig.. 13: MSE performance of CFO estimates for four repetitions, true CFO=0:93 subcarrier spacings.